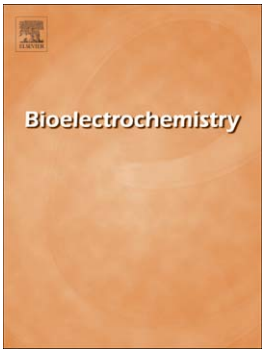

Aptamer based electrochemical biosensor for detection of adenosine triphosphate using a nanoporous gold platform

Leila Kashefi-Kheyrabadi, Masoud A. Mehrgardi

PII: S1567-5394(13)00056-X
DOI: doi: 10.1016/j.bioelechem.2013.05.005
Reference: BIOJEC 6681

To appear in: *Bioelectrochemistry*

Received date: 4 March 2013
Revised date: 26 May 2013
Accepted date: 29 May 2013

Please cite this article as: Leila Kashefi-Kheyrabadi, Masoud A. Mehrgardi, Aptamer based electrochemical biosensor for detection of adenosine triphosphate using a nanoporous gold platform, *Bioelectrochemistry* (2013), doi: 10.1016/j.bioelechem.2013.05.005

Aptamer based electrochemical biosensor for detection of adenosine triphosphate using a nanoporous gold platform

Leila Kashefi-Kheyrabadi, Masoud A. Mehrgardi*

Department of chemistry, University of Isfahan, Isfahan, 81746-73441, Iran

Abstract

In spite of the promising applications of aptamers in the bioassays, the development of aptamer-based electrochemical biosensors with the improved limit of detection has remained a great challenge. A strategy for the amplification of signal, based on application of nanostructures as platforms for the construction of an electrochemical adenosine triphosphate (ATP) aptasensor, is introduced in the present manuscript. A sandwich assay is designed by immobilizing a fragment of aptamer on a nanoporous gold electrode (NPGE) and its association to second fragment in the presence of ATP. Consequently, 3, 4-diaminobenzoic acid (DABA), as a molecular reporter, is covalently attached to the amine-label of the second fragment, and the direct oxidation signal of DABA is followed as the analytical signal. The sensor can detect the concentrations of ATP as low as submicromolar scales. Furthermore, 3.2% decrease in signal is observed by keeping the aptasensor at 4^{o}C for a week in buffer solution, implying a desirable stability. Moreover, analogue nucleotides, including GTP, UTP and CTP, do not show serious interferences and this sensor easily detects its target in deproteinized human blood plasma.

Keywords: Aptasensor, Aptamer, Adenosine triphosphate, Nanoporous gold electrode, 3, 4-diaminobenzoic acid.

*Author to whom correspondence should be addressed: m.mehrgardi@chem.ui.ac.ir

Tel: +98-311-7932710

Fax: +98-311-6689732

1. Introduction

A wide variety of nanoscale materials with diverse sizes, shapes and structures are now available. The amazingly small sizes and desirable properties of nanomaterials make them very attractive tools to investigate for various fields of science [1]. They play important roles in construction of high-performance bioassays to detect target molecules using different analytical methods. Owing to prominent properties, such as high specific surface area, well-ordered pore structures, excellent conductivity, biocompatibility, chemical and thermal stability, mechanical strength and toxicological safety, gold nanoporous materials are attractive supports for the adsorption or immobilization of biocomponents in confined spaces at the nanoscale [2-4]. They have been used for catalysis [5], energy storage [6], enzymatic assays [7, 8] and development of biosensors [9, 10]. Preparation of gold porous substrates have been accomplished using different methods such as template-directed synthesis [7], hydrothermal treatment [11], electrochemical/chemical dealloying [12, 13]. Recently, some new facile electrochemical strategies have been reported to fabricate NPGEs [14-16]. All these methods prepare NPGE using in-situ procedure. As a nanotructured biointerface, in-situ prepared NPGE is very appropriate for the construction of electrochemical biosensors due to its easy manipulation and high stability.

Aptamers are nucleic acid-based ligands that are being used in various novel scientific fields. They are characterized by a versatile selection process, high affinity and specificity for their targets, simplicity of synthesis and finally rapid production processes. Aptamers can be stored long term at ambient temperature and can sustain reversible denaturation [17]. All these properties collectively make them ideal to apply in bioelectrochemical assays. Up to now, various aptamer-based sensors (aptasensors) have been reported for the widespread range of targets, including small molecules [18], pharmaceutical drugs [19], biological macromolecules [20], and even whole cells [4]. Among them, electrochemical aptasensors have attracted interests, due to their combined advantages of sensitivity, miniaturization capability, minimal power requirement, and low cost, as well as high stability [21-23].

Electrochemical aptasensors for detection of small molecules such as ATP and cocaine have been recently developed [24-26]. ATP is a vital substrate in living organisms and as an indicator for the cell viability and the cell injury [27, 28]. It is well- known as the mediator of energy exchanges in all living cells [29]. This small molecule plays a key role in cell metabolism, which is involved in many metabolic processes [30, 31]. Detection of ATP with low-affinity aptamer leads to be more challenging than the other targets with well-known high-affinity aptamers. From this view, detection of ATP using innovative strategies is very attractive.

In this manuscript, a NPGE-based aptasensor for detection of ATP using DABA as a molecular reporter is described. DABA was previously used to quantify DNA and determination of DNA–protein interaction by fluorometric methods [32, 33]. In the present study, for constructing the nanostructured aptasensor, a well-known ATP binding aptamer splits into two fragments [26, 34]. The first fragment is immobilized onto NPGE via alkane thiol self-assembled monolayer chemistry. Subsequently, the second fragment is covalently bound to the activated carboxylic group of the molecular reporter using EDC/NHS chemistry. In the presence of ATP, two fragments of aptamer associate together.

Consequently, this increases the concentration of DABA at the electrode surface and can be easily monitored using electrochemical techniques.

2. Experimental

2.1. Chemicals

DABA, Hexaammineruthenium(III) chloride (RuHex), ascorbic acid, magnesium chloride, sodium chloride, potassium chloride, sodium dihydrogen phosphate, disodium hydrogen phosphate, 1-ethyl-3-(3 dimethylaminopropyl) carbodiimidehydrochloride (EDC), N-hydroxysuccinimide (NHS), tris-(2-carboxyethyl) phosphine hydrochloride (TCEP), potassium ferrocyanide, potassium ferricyanide, nitric acid and sulfuric acid were purchased from commercial sources (Merck or Sigma) in analytical grade. ATP, guanosine triphosphate (GTP), cytidine triphosphate (CTP), and uridine triphosphate (UTP) were obtained from Vivantis Co. (Malaysia). Amino labeled oligonucleotides and thiolated oligonucleotides were obtained from Eurofins MWG/Operon Co. with following sequences:

F1: 5'-HS-(CH2)6-ACCTGGGGGAGTAT-3';

F2: 5'-TGCGGAGGAAGGT-(CH2)2-NH2-3'

All chemicals were used as received. The stock solutions of the aptamers (4.0 μM) were prepared using PBS buffer solution (pH=7.0) and kept at −20°C. Serum samples of healthy human volunteer blood donations were obtained from Esfahan Blood Transfusion Organization (EBTO). The distilled deionized (DI) water (R=18 MΩ) was used in all solution preparations.

2.2. Instrumentation

Electrochemical experiments were carried out using an Autolab PGSTAT30 (ECOchemie, The Netherlands, driven by GPES 4.9 software). A conventional three-electrode system, consisting of small parts of gold recordable compact disks (CD-R) as a working electrode, a platinum wire as an auxiliary electrode and an Ag/AgCl/3.0 M KCl as a reference electrode was used for all experiments. The differential pulse voltammograms have been recorded at the scan rate of 10 mV s^{-1} and the pulse amplitude of 25 mV. Electrochemical impedance spectroscopy (EIS) experiments were accomplished at a constant DC potential of +0.23 V. The applied AC potential was 5 mV. Chronocoulometry experiments were performed at pulse duration of 500 ms and pulse amplitude of 500 mV. All experiments were performed at room temperature. Scanning electron microscopy (SEM, Philips L33) was used to characterize the morphology of the electrode.

2.3. Preparation of NPGE

Prior to NPGE preparation, the gold electrode is prepared using a CD-R according to previously reported procedures [15, 35, 36]. Concisely, a piece of CD-R is cut and the protective layer is removed by putting it in the concentrated nitric acid. Afterward, it is rinsed by DI water thoroughly; then, it is fixed to the bottom of a Teflon cell with an O-ring and is used as the working electrode.

In the next step, NPGE is prepared during two steps. In the first step, the gold electrode is anodized in a 0.2 M phosphate buffer solution (pH=7.4) for 3 minutes by applying a step potential from the open-circuit potential (OCP) to 4V. Gas bubbles are produced on the gold surface during anodizing process. While gas evolution is accomplished an oxide film is grown on the gold substrate until the anodizing process is terminated. Under these conditions only oxygen evolution can be done and the produced bubbles at the anode are oxygen [15]. At the next step, ascorbic acid is applied as a non-toxic and low-cost reducing agent to reduce gold oxide to metallic Au. The reduction is performed by incubating the anodized gold substrate in a 1.0 M ascorbic acid solution for 3 minutes. Due to its high surface area and nanometer crystal size, the color of the gold surface changes to dark [37].

2.4. Nanoporous platform modification

Fig. 1 shows the different steps of fabrication of the gold nanoporous-based aptasensor.

Prior to sensor fabrication, for reduction of the disulfide bond of F1 fragment, a 20.0 µL aliquot of 4.0 µM F1 with 5.0 µL of 0.5 mM TCEP is incubated in darkness for 1 h. Afterward, it is self-assembled onto NPGE surface by dropping 15.0 µL of 4.0 µM F1 solution and 12.0 µL of 2.0 M magnesium chloride for 24 h. Then, the electrode is thoroughly rinsed with DI water and stored in 10 mM phosphate buffer (pH 7.0) prior to use.

For monitoring the response of the sensor to different concentration of ATP, the second fragment of aptamer should associate to the immobilized fragment on the surface in the presence of ATP and then a molecular reporter is covalently bound to this fragment. For this purpose, 15.0 µL ATP (various concentrations) and 15.0 µL of 4.0 µM F2 fragment are dropped onto NPGE simultaneously for 5 minutes. It was found that the optimum time for aptamer fragments interaction is equal to 5 minutes (Fig.S1). Afterward, the modified electrode is rinsed by DI water. Finally, a 0.1 M phosphate buffer solution (pH=7.4) containing 1.0 mM DABA as molecular reporter, 20 mM of EDC and 30 mM of NHS is dropped onto the electrode surface for 2 h for the covalently attachment of DABA to be amino-label of F2. The resulting electrode is ready for the electrochemical detection.

EIS is applied to follow different modification steps. For EIS analysis, a solution of 0.5 mM potassium ferricyanide and potassium ferrocyanide (1:1) in 0.1M KCl is used. The differential

pulse voltammetry (DPV) responses of DABA are followed as an analytical signal. DPV experiments are done in 0.05 M phosphate buffer solution (pH 5.5).

Here Fig.1

3. Results and discussion

In this manuscript, the effect of nanoporous structure of the electrode surface on the detection sensitivity of an electrochemical ATP aptasensor, which uses DABA as a molecular reporter, is investigated. An in-vitro selected 27-mer ATP binding aptamer (ABA), which owns high selectivity for ATP against its analogues, GTP, CTP, and UTP is employed. ABA is split into two fragments according to the previously reported manuscripts [26, 34]. These two fragments fold around ATP molecules on the surface of NPGE and from an associated complex, which creates a sandwich assay aptasensor for the detection of ATP. Associated second fragment is modified by DABA and electrochemical oxidation of DABA is followed as the analytical signal. The active surface area of the electrode and consequently the loading of F1- aptamers are increased by converting it to nanoporous structure. Therefore, more ATP, F2- aptamer, and DABA are accumulated onto the surface. By more loading of DABA molecules on the surface, the signal is amplified.

3.1. Characterization of NPGE

To compare the electrochemically active surface area of smooth gold electrode and NPGE, cyclic voltammograms of both electrodes are recorded in 0.1 M H_2SO_4 in the same condition. As Fig. 2 shows, both electrodes represent a symmetric cathodic peak at ~0.8 V, arising by the electrochemical reduction of gold oxide formed during the anodic scan. However, the reduction peak current of NPGE is significantly higher than that observes on the smooth gold surface due to larger surface area. By assuming 386 $\mu C.cm^{-2}$ required charges for the reduction of one monolayer of gold oxide to metallic gold [38], the real surface area of the smooth gold electrode and NPGE are obtained equal to 0.22 ± 0.01 cm^2 and 1.9 ± 0.10 cm^2, respectively. These values represent approximately a nine-fold increase in the surface area after electrode processing. Fig. 3 shows scanning electron microscopic image of both NPGE and smooth gold electrodes. The surface micrograph of NPGE reveals a nanoporous structure, while that of gold substrate shows a smooth structure. The observed parallel channels in SEM images are the grooves on recordable CD.

Here Fig.2

Here Fig.3

3.2. Electrochemical characterization of sensing interface

The biorecognition layer on the electrode surface is characterized using EIS and voltammetric techniques. EIS not only is applied as a very powerful method for the characterization of sensing interfaces, but it also provides a suitable transduction technique to follow the interfacial interactions of biomolecules [39]. One of the favorable properties of EIS is nondestructive character of this technique that makes it extremely attractive for the electrochemical biosensing assays [23, 40-42]. The capacitance and resistance properties of the solid support-electrolyte interface change by the immobilization of biomolecules on the conductive or semi-conductive supports [39]. Actually, the presence of biomaterial films on the electrode surface decreases the double-layer capacitance and retards the interfacial electron-transfer kinetics [43]. These effects depend on the molecular and immobilization characteristics of the recognition layer on the surface.

The impedance spectra at the different steps of electrode surface modification are shown in Fig. 4. F1 immobilization on the NPGE surface causes an increase in the charge transfer resistance (R_{ct}). To optimize the immobilization amount of F1 fragment, various concentrations of F1 aptamer (2-10 μM) have been self-assembled on NPGE surface. The impedance spectra (Fig.S2) demonstrated that the immobilization of F1 is increased by increasing of F1 concentration up-to 4.0 μM and for further experiments 4.0 μM was applied as optimum concentration. In the next step, association of F1 and F2 in the presence of ATP causes a significant increase in the charge resistance. These changes arise by blocking of the electrode surface by both electrostatic repulsion between the negatively charged redox indicator $[Fe(CN)6]^{3-/4-}$ and the phosphate backbone of ABA fragments and also spatial restriction of ABA. The R_{ct} is 250 ± 50, 3000 ± 270, 3600 ±300 and 6500±450 Ω for NPGE, after F1 immobilization and F2 association in the absence and presence of 1.0 mM ATP, respectively. This is in consistent with previously published report [44].

Here Fig.4

Modification of the electrode surface is also followed using cyclic voltammetry. Fig. 5 shows the cyclic voltammograms of potassium ferricyanide on the NPGE and modified electrode for each step of the modification. As Fig. 5 shows, due to the development of negative charges on the surface of the electrode, immobilization of F1 onto the NPGE surface causes a decrease in the faradic peak current (I_p) and an increase in the peak potential separation (ΔE_p). As a result of the F2 association with F1 in the presence of ATP, a sandwich structure is formed onto the NPGE. Consequently, aptamer layer on the electrode surface becomes denser and the negative charge of the electrode surface increases more than the previous step. Therefore, the approachability of negatively charged ferricyanide ions to the electrode surface becomes difficult, the peak potential separation (ΔEp) increases and the faradic peak current (Ip) more decrease (Fig. 5). These changes are in good agreement with EIS results.

Here Fig.5

3.3. Quantitation of aptamer surface density

Aptamer coverage at the electrode surface can be estimated using cationic redox molecules that electrostatically associated with the negatively charged aptamer backbone [45]. Cations provide charge compensation for the anionic phosphate groups in aptamer backbone. Briefly, the modified NPGE with aptamer is incubated in the 50mM RuHex solution with low ionic strength (0.05M KCl). The amount of cationic redox probe, RuHex, is then measured by chronocoulometric technique, under equilibrium condition [46]. By referring to the Cottrell equation, the chronocoulometric intercept at t=0 is sum of the double layer charge and the charge due to the reaction of redox probe that accumulate on the electrode surface by adsorbing onto the phosphate backbone of F1. The surface excess terms are calculated by the difference between the chronocoulometric intercepts for the identical potential step experiments in the presence and in the absence of the redox probe. Aptamer surface density can be estimated using the following equation:

$$\Gamma_{apt} = \Gamma_0(z/m)$$

Where Γ_{apt} is the aptamer surface density in mol/cm^2, m is the number of bases in aptamer and z is the charge of RuHex. Finally the surface density of aptamer is obtained equal to 14 ± 0.4 pmol cm^{-2} (n=3).

3.4. Analytical performance of the aptasensor

CV was applied for the investigation of electrochemical behavior of DABA. Fig. 6 shows the cyclic voltammograms of 1.0 mM of DABA in 0.05 M phosphate buffer solution at pH 5.5. The voltammogram shows a well-known anodic peak at ~0.47 V in the first scan, but in the second scan, another anodic peak is observed at ~0.12 V. This peak can be corresponded to the formation of DABA oligomer by the oxidation of DABA during the first scan [47].

Here Fig.6

In this research, two fragments of ABA are associated on the NPGE surface in the presence of ATP, and then F2 is modified by DABA. The oxidation peak of DABA is shifted to more

positive potentials (~0.17V) and followed as the analytical signal. The oxidation peak currents of DABA not only depend on the concentration of ATP, but also depend on the concentration of F2-DABA. The lower concentrations of F2 destabilize the associated complex; and their higher concentration causes to form more associated complex in the absence of ATP, and therefore, more background currents are observed and so the signal increase percentage will be decreased. It was found that the optimum concentration of F2 for the proposed aptasensor is equal to 4.0 μM (Fig. 7). Under optimum conditions, by addition of ATP, more F2 fragment associates to F1. This causes large increase in faradic current. Fig. 8 shows a monotonic increase in peak currents with increasing ATP concentrations until saturation at the concentrations up to 3mM ATP. This aptasensor easily detects ATP at concentrations as low as 100 nM (Fig. 9). Detection sensitivity of the aptasensor compares favorably with other previously reported ATP aptasensors [24, 26].

Here Fig.7

Here Fig.8

Here Fig.9

3.5. Selectivity, stability and reproducibility

The selectivity of the aptasensor is investigated by following the DABA oxidation signal when the sensor treated with other nucleotide analogues including UTP, GTP, and CTP (all of 1.0 mM concentrations) instead of ATP. The oxidation peak currents of DABA for the ATP analogues are roughly as low as the signal in the absence of ATP, ~80-fold lower than that is seen for 1.0 mM ATP (Table 1). The introduced aptasensor shows excellent specific response against ATP analogues. This result obviously confirms the fact that the NPGE design does not change the selectivity of the ATP aptamer.

Furthermore, in order to investigate the ability of the aptasensor to detect ATP under realistic conditions, it was applied to the human blood plasma sample. To avoid nonspecific adsorption of proteins on the surface of NPGE, the plasma is pretreated upon previously reported procedure [48]. Briefly, it is deproteinized by trichloroacetic acid and diluted 10- folds using 10.0 mM phosphate buffer (pH 7.0). Subsequently, ATP is spiked into the pretreated plasma and it employs as a working solution in the electrochemical experiments. As table 1 shows ATP aptasensor strongly supports the detection of its target even in the complicated matrix under realistic conditions.

The stability of the aptasensor is examined by incubation of the F1-modified electrode in PBS 1X (pH 7.0) at 4 °C. After 1 week, 3.2% decrease is observed for the detection of the same ATP concentration (Fig.S3) implying good electrode stability.

In order to evaluate the inter-day variations of the aptasensor, a series of three electrodes is examined for the detection of 1.0 mM ATP. The relative standard deviation (RSD) of 3.3% for these experiments is obtained. This shows the reproducibility of the aptasensor is quite reliable.

Here Table 1

4. Conclusions

A strategy based on nanostructure platform for the signal amplification of an electrochemical ATP aptasensor using DABA as a molecular reporter is demonstrated in this manuscript. The introduced assay combines several advantages simultaneously; first, it is essentially resistant to nonspecific interferences and usable in a complex media such as human blood plasma in compared to other electrochemical sensors [49-51]. Second, it can detect the concentrations of ATP at sub-micromolar scales. Third, it is a signal-on sensor, with acceptable stability. At last but not least, it is prepared by a fairly easy procedure. The emergence of NPGE introduces a promising strategy in aptasensor field. It could be extended to fabricate sensitive biosensor for the detection of other targets even whole cells.

Acknowledgments

The authors gratefully appreciate the financial support for this project by the research council of the University of Isfahan. Also we would like to express our sincere acknowledgments to Esfahan Blood Transfusion Organization (EBTO) for providing serum samples of healthy human volunteer blood donations.

References

[1] K.E. Gonsalves, C.R. Halberstadt, C.T. Laurencin, L.S. Nair, Biomedical Nanostructures, John Wiley & Sons, pp. 5-20.

[2] H. Qiu, L. Xue, G. Ji, G. Zhou, X. Huang, Y. Qu, P. Gao, Enzyme-modified nanoporous gold-based electrochemical biosensors, *Biosens. Bioelectron.* 24 (2009) 3014-3018.

[3] K. Hu, P. Liu, S. Ye, S. Zhang, Ultrasensitive electrochemical detection of DNA based on PbS nanoparticle tags and nanoporous gold electrode, *Biosens. Bioelectron.* 24 (2009) 3113-3119.

[4] H. Qiu, Y. Sun, X. Huang, Y. Qu, A sensitive nanoporous gold-based electrochemical aptasensor for thrombin detection, *Colloids Surf. B. Biointerfaces* 79 (2010) 304-308.

[5] C. Xu, J. Su, X. Xu, P. Liu, H. Zhao, F. Tian, Y. Ding, Low Temperature CO Oxidation over Unsupported Nanoporous Gold, *J. Am. Chem. Soc.* 129 (2006) 42-43.

[6] Y. Ding, M. Chen, J. Erlebacher, Metallic Mesoporous Nanocomposites for Electrocatalysis, *J. Am. Chem. Soc.* 126 (2004) 6876-6877.

[7] H. Qiu, Y. Li, G. Ji, G. Zhou, X. Huang, Y. Qu, P. Gao, Immobilization of lignin peroxidase on nanoporous gold: Enzymatic properties and in situ release of H2O2 by co-immobilized glucose oxidase, *Bioresour. Technol.* 100 (2009) 3837-3842.

[8] G.B. Stevens, T. Reda, B. Raguse, Energy storage by the electrochemical reduction of CO2 to CO at a porous Au film, *J. Electroanal. Chem.* 526 (2002) 125-133.

[9] H.-J. Qiu, G.-P. Zhou, G.-L. Ji, Y. Zhang, X.-R. Huang, Y. Ding, A novel nanoporous gold modified electrode for the selective determination of dopamine in the presence of ascorbic acid, *Colloids Surf. B. Biointerfaces* 69 (2009) 105-108.

[10] H. Qiu, C. Xu, X. Huang, Y. Ding, Y. Qu, P. Gao, Immobilization of Laccase on Nanoporous Gold: Comparative Studies on the Immobilization Strategies and the Particle Size Effects, *J. Phys. Chem. C.* 113 (2009) 2521-2525.

[11] A. Huczko, Template-based synthesis of nanomaterials, *Appl. Phys. A: Mater. Sci. Process.* 70 (2000) 365-376.

[12] Q. Yi, W. Yu, Nanoporous gold particles modified titanium electrode for hydrazine oxidation, *J. Electroanal. Chem.* 633 (2009) 159-164.

[13] J.F. Huang, I.W. Sun, Fabrication and Surface Functionalization of Nanoporous Gold by Electrochemical Alloying/Dealloying of Au–Zn in an Ionic Liquid, and the Self-Assembly of L-Cysteine Monolayers, *Adv. Funct. Mater.* 15 (2005) 989-994.

[14] W. Huang, M. Wang, J. Zheng, Z. Li, Facile Fabrication of Multifunctional Three-Dimensional Hierarchical Porous Gold Films via Surface Rebuilding, *J. Phys. Chem. C.* 113 (2009) 1800-1805.

[15] A. Kiani, E.N. Fard, Fabrication of palladium coated nanoporous gold film electrode via underpotential deposition and spontaneous metal replacement: A low palladium loading electrode with electrocatalytic activity, *Electrochim. Acta* 54 (2009) 7254-7259.

[16] H. Qiu, X. Huang, Effects of Pt decoration on the electrocatalytic activity of nanoporous gold electrode toward glucose and its potential application for constructing a nonenzymatic glucose sensor, *J. Electroanal. Chem.* 643 (2010) 39-45.

[17] E. Levy-Nissenbaum, A.F. Radovic-Moreno, A.Z. Wang, R. Langer, O.C. Farokhzad, Nanotechnology and aptamers: applications in drug delivery, *Trends Biotechnol.* 26 (2008) 442-449.

[18] D. Ho, K. Falter, P. Severin, H.E. Gaub, DNA as a Force Sensor in an Aptamer-Based Biochip for Adenosine, *Anal. Chem.* 81 (2009) 3159-3164.

[19] L. Kashefi-Kheyrabadi, M.A. Mehrgardi, Design and construction of a label free aptasensor for electrochemical detection of sodium diclofenac, *Biosens. Bioelectron.* 33 (2012) 184-189.

[20] D.T. Tran, V. Vermeeren, L. Grieten, S. Wenmackers, P. Wagner, J. Pollet, K.P.F. Janssen, L. Michiels, J. Lammertyn, Nanocrystalline diamond impedimetric aptasensor for the label-free detection of human IgE, *Biosens. Bioelectron.* 26 (2011) 2987-2993.

[21] X. Yu, C.M. Valmikinathan, A. Rogers, J. Wang, Nanotechnology and Drug Delivery in: Biomedical Nanostructures, John Wiley & Sons, 2007, pp. 93-113.

[22] A.A. Lubin, R.Y. Lai, B.R. Baker, A.J. Heeger, K.W. Plaxco, Sequence-specific, electronic detection of oligonucleotides in blood, soil, and foodstuffs with the reagentless, reusable E-DNA sensor, *Anal. Chem.* 78 (2006) 5671-5677.

[23] A.E. Radi, J.L. Acero Sanchez, E. Baldrich, C.K. O'Sullivan, Reusable impedimetric aptasensor, *Anal. Chem.* 77 (2005) 6320-6323.

[24] X. Zuo, S. Song, J. Zhang, D. Pan, L. Wang, C. Fan, A Target-Responsive Electrochemical Aptamer Switch (TREAS) for Reagentless Detection of Nanomolar ATP, *J. Am. Chem. Soc.* 129 (2007) 1042-1043.

[25] Z. Tang, P. Mallikaratchy, R. Yang, Y. Kim, Z. Zhu, H. Wang, W. Tan, Aptamer Switch Probe Based on Intramolecular Displacement, *J. Am. Chem. Soc.* 130 (2008) 11268-11269.

[26] X. Zuo, Y. Xiao, K.W. Plaxco, High Specificity, Electrochemical Sandwich Assays Based on Single Aptamer Sequences and Suitable for the Direct Detection of Small-Molecule Targets in Blood and Other Complex Matrices, *J. Am. Chem. Soc.* 131 (2009) 6944-6945.

[27] H.J. Agteresch, P.C. Dagnelie, J.W.O. van den Berg, J.H.P. Wilson, Adenosine Triphosphate: Established and Potential Clinical Applications, *Drugs* 58 (1999) 211-232.

[28] F. Yu, L. Li, F. Chen, Determination of adenosine disodium triphosphate using prulifloxacin–terbium(III) as a fluorescence probe by spectrofluorimetry, *Anal. Chim. Acta* 610 (2008) 257-262.

[29] T. Pérez-Ruiz, C. Martínez-Lozano, V. Tomás, J. Martín, Determination of ATP via the photochemical generation of hydrogen peroxide using flow injection luminol chemiluminescence detection, *Anal. Bioanal. Chem.* 377 (2003) 189-194.

[30] Q. Deng, I. German, D. Buchanan, R.T. Kennedy, Retention and Separation of Adenosine and Analogues by Affinity Chromatography with an Aptamer Stationary Phase, *Anal. Chem.* 73 (2001) 5415-5421.

[31] D.E. Huizenga, J.W. Szostak, A DNA aptamer that binds adenosine and ATP, *Biochemistry* 34 (1995) 656-665.

[32] A. Pestaña, R. Castro, J. Castell, R. Marco, Fluorometric assays in the study of nucleic acid-protein interactions: I. The use of diaminobenzoic acid as a reagent of DNA, *Anal. Biochem.* 90 (1978) 543-550.

[33] P.S. Thomas, M.N. Farquhar, Specific measurement of DNA in nuclei and nucleic acids using diaminobenzoic acid, *Anal. Biochem.* 89 (1978) 35-44.

[34] Y. Lu, X. Li, L. Zhang, P. Yu, L. Su, L. Mao, Aptamer-Based Electrochemical Sensors with Aptamer−Complementary DNA Oligonucleotides as Probe, *Anal. Chem.* 80 (2008) 1883-1890.

[35] L. Angnes, E.M. Richter, M.A. Augelli, G.H. Kume, Gold Electrodes from Recordable CDs, *Anal. Chem.* 72 (2000) 5503-5506.

[36] A.A.P. Ferreira, C.S. Fugivara, S. Barrozo, P.H. Suegama, H. Yamanaka, A.V. Benedetti, Electrochemical and spectroscopic characterization of screen-printed gold-based electrodes modified with self-assembled monolayers and Tc85 protein, *J. Electroanal. Chem.* 634 (2009) 111-122.

[37] F. Jia, C. Yu, K. Deng, L. Zhang, Nanoporous Metal (Cu, Ag, Au) Films with High Surface Area: General Fabrication and Preliminary Electrochemical Performance, *J. Phys. Chem. C.* 111 (2007) 8424-8431.

[38] R. Szamocki, A. Velichko, C. Holzapfel, F. Mücklich, S. Ravaine, P. Garrigue, N. Sojic, R. Hempelmann, A. Kuhn, Macroporous Ultramicroelectrodes for Improved Electroanalytical Measurements, *Anal. Chem.* 79 (2006) 533-539.

[39] E. Katz, I. Willner, Probing Biomolecular Interactions at Conductive and Semiconductive Surfaces by Impedance Spectroscopy: Routes to Impedimetric Immunosensors, DNA-Sensors, and Enzyme Biosensors, *Electroanalysis* 15 (2003) 913-947.

[40] J. Elbaz, B. Shlyahovsky, D. Li, I. Willner, Parallel Analysis of Two Analytes in Solutions or on Surfaces by Using a Bifunctional Aptamer: Applications for Biosensing and Logic GateOperations, Chembiochem 9 (2008) 232-239.

[41] M.C. Rodriguez, A.N. Kawde, J. Wang, Aptamer biosensor for label-free impedance spectroscopy detection of proteins based on recognition-induced switching of the surface charge, *Chem. Commun.* (2005) 4267-4269.

[42] M. Zayats, Y. Huang, R. Gill, C.A. Ma, I. Willner, Label-free and reagentless aptamer-based sensors for small molecules, *J. Am. Chem. Soc.* 128 (2006) 13666-13667.

[43] J.S. Daniels, N. Pourmand, Label-Free Impedance Biosensors: Opportunities and Challenges, *Electroanalysis* 19 (2007) 1239-1257.

[44] Y. Fu, R. Yuan, L. Xu, Y. Chai, X. Zhong, D. Tang, Indicator free DNA hybridization detection via EIS based on self-assembled gold nanoparticles and bilayer two-dimensional 3-mercaptopropyltrimethoxysilane onto a gold substrate, *Biochem. Eng. J.* 23 (2005) 37-44.

[45] A.B. Steel, T.M. Herne, M.J. Tarlov, Electrochemical Quantitation of DNA Immobilized on Gold, *Anal. Chem.* 70 (1998) 4670-4677.

[46] A.J. Bard, L.R. Faulkner, Electrochemical methods: fundamentals and applications, Wiley, 2001.

[47] I. Losito, F. Palmisano, P.G. Zambonin, o-Phenylenediamine Electropolymerization by Cyclic Voltammetry Combined with Electrospray Ionization-Ion Trap Mass Spectrometry, *Anal. Chem.* 75 (2003) 4988-4995.

[48] J.M. Berg, J.L. Tymoczko, L. Stryer, Biochemistry, 5th ed., W.H. Freeman, New York, 2002.

[49] C. Fan, K.W. Plaxco, A.J. Heeger, Electrochemical interrogation of conformational changes as a reagentless method for the sequence-specific detection of DNA, *Proc. Natl. Acad. Sci.* 100 (2003) 9134-9137.

[50] Y. Xiao, A.A. Lubin, A.J. Heeger, K.W. Plaxco, Label-Free Electronic Detection of Thrombin in Blood Serum by Using an Aptamer-Based Sensor, *Angew. Chem. Int. Ed.* 44 (2005) 5456-5459.

[51] Y. Xiao, B.D. Piorek, K.W. Plaxco, A.J. Heeger, A Reagentless Signal-On Architecture for Electronic, Aptamer-Based Sensors via Target-Induced Strand Displacement, *J. Am. Chem. Soc.* 127 (2005) 17990-17991.

Table 1. ATP sensor responses for 1 mM solutions of ATP, UTP, CTP and GTP and also for 1 mM ATP spiked to pretreated plasma (PT-Plasma).

Target	Ip/μA	SD
UTP	0.05	0.03
CTP	0.05	0.02
GTP	0.03	0.02
ATP(buffer)	2.35	0.08
ATP(PT-Plasma)	2.15	0.1

Figure captions:

Fig. 1 Schematic presentation of different modification steps for fabrication of the gold nanoporous-based aptasensor.

Fig. 2 Cyclic voltammograms on (a) smooth gold electrode and (b) NPGE in 0.1M H_2SO_4 at scan rate 100 mV s^{-1}

Fig. 3 SEM images of (a) smooth gold and (b) nanoporous gold electrodes.

Fig. 4 Electrochemical impedance spectra of different modification steps: (a) NPGE (b) NPGE /F1 (c) NPGE /F1/F2 and (d) NPGE /F1 /ATP (1mM)/F2 in a solution containing $[Fe(CN)_6]^{3-/4-}$ (5×10^{-4} M; 1:1) as a redox probe at a constant DC potential of +0.23V.

Fig. 5 Cyclic voltammograms of (a) NPGE, (b) NPGE /F1, (c) NPGE /F1/F2 and (d) NPGE /F1 /ATP (1mM)/F2 in a solution containg $[Fe(CN)6]^{3-}$ (5×10^{-4} M) and 0.1 M KCl at scan rate of 100 mV s^{-1}

Fig. 6. Cyclic voltammograms of 1 mM DABA in 0.05 M phosphate buffer solution (pH 5.5) at scan rate of 50 mV s^{-1} (a) first scan and (b) second scan.

Fig.7 The percentage of signal increases for different concentration of F2 fragment in the presence of 1 mM ATP. The data points and error bars correspond to the average and standard deviations from three independently fabricated electrodes.

Fig.8. Differential pulse voltammograms of ATP aptasensor in the presence of various concentrations of ATP (0, 0.1, 1, 10, 100, 500, 1000, 2000, 3000 μM) at scan rate of 10 mV s^{-1} and pulse amplitude 25 mV.

Fig.9. Peak current responses of ATP aptasensor vs. logarithm of ATP concentrations. The data points and error bars correspond to the average and standard deviations from three independently measurements.

Fig.1.

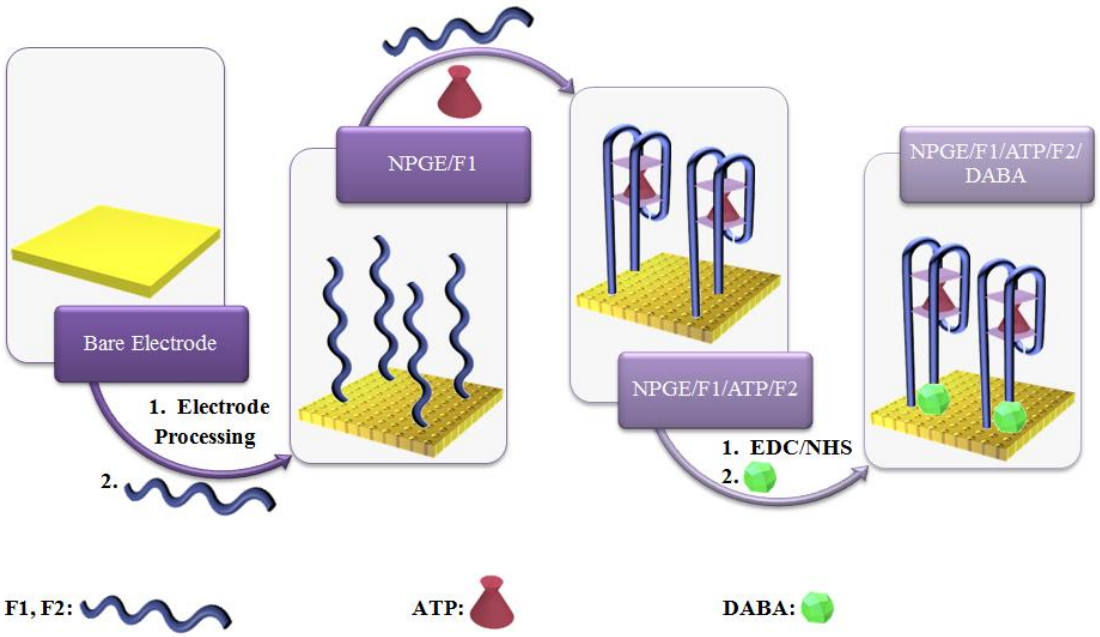

Fig. 2.

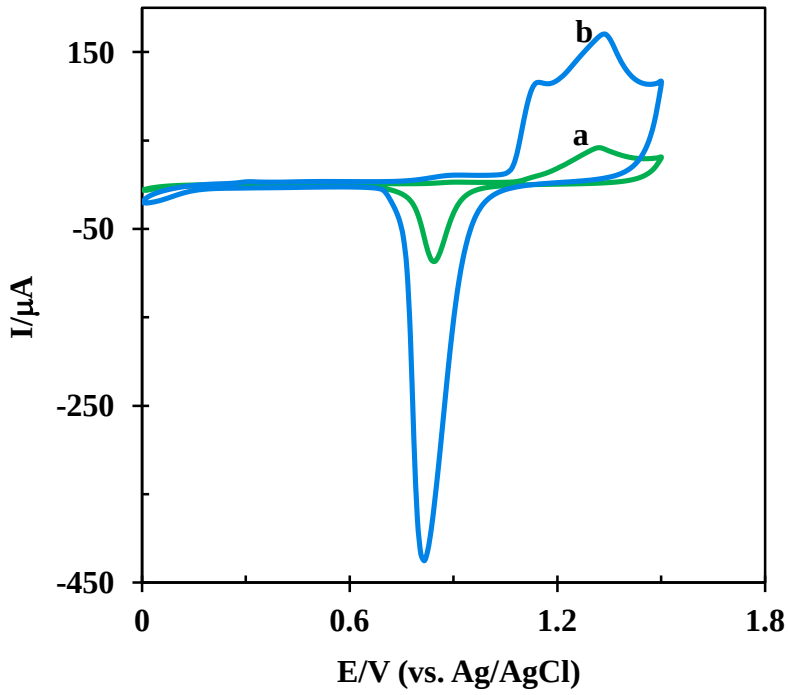

Fig.3.

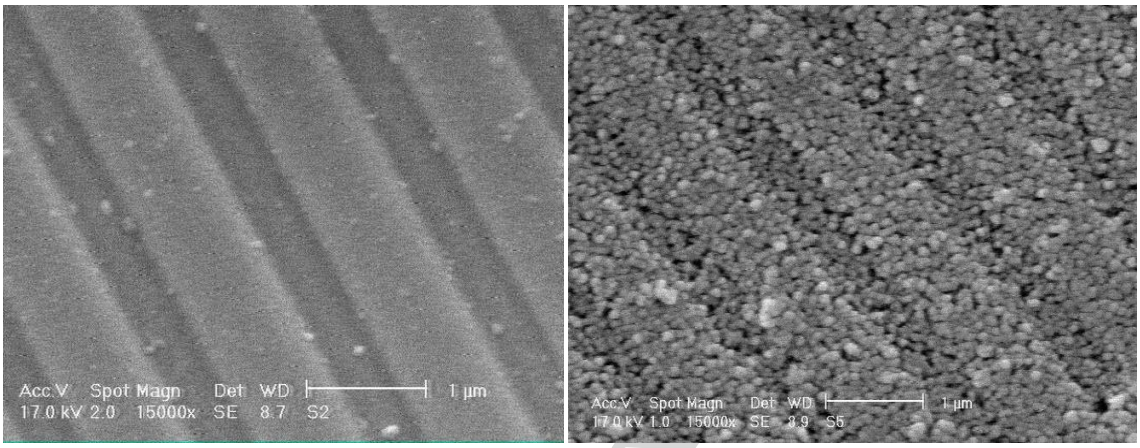

Fig. 4.

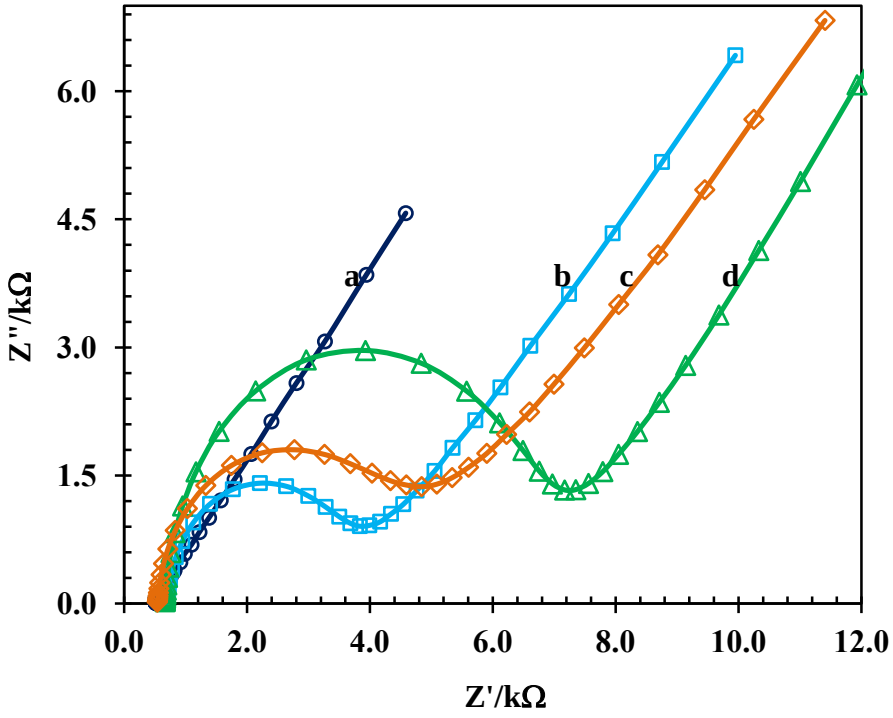

Fig. 5.

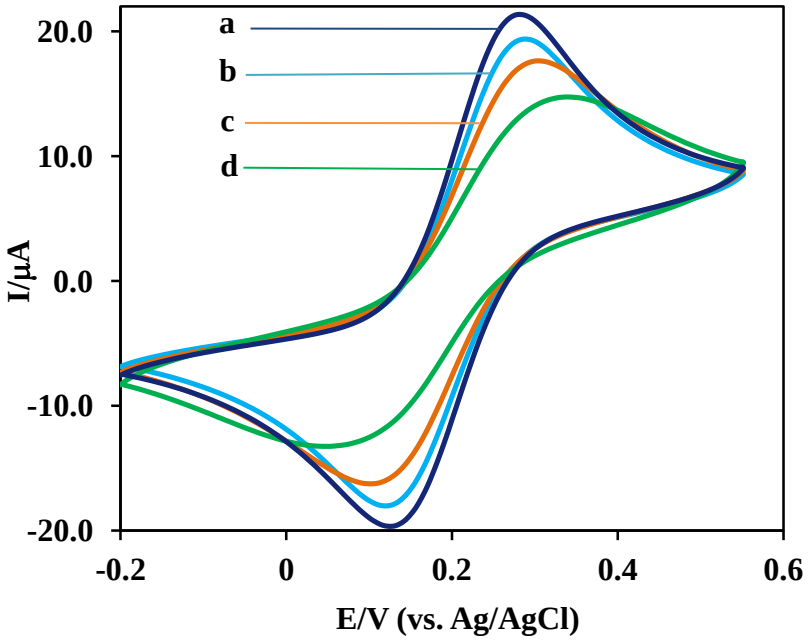

Fig. 6.

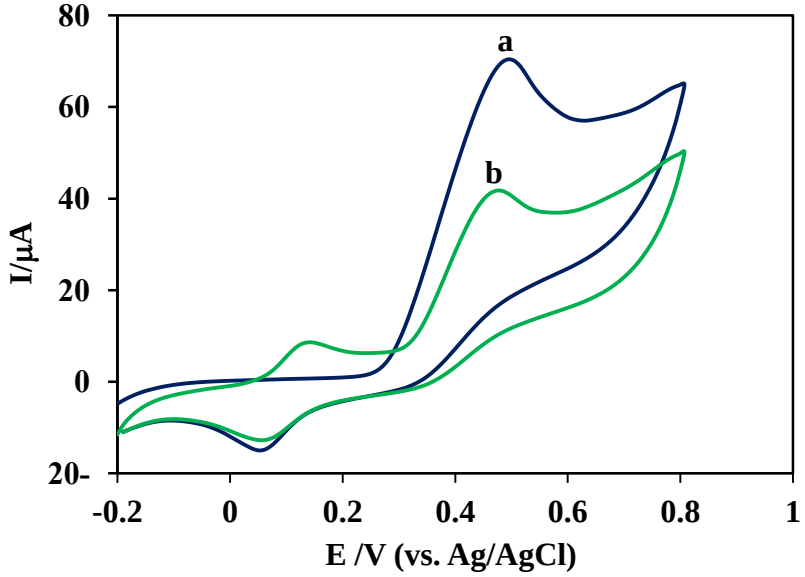

Fig. 7.

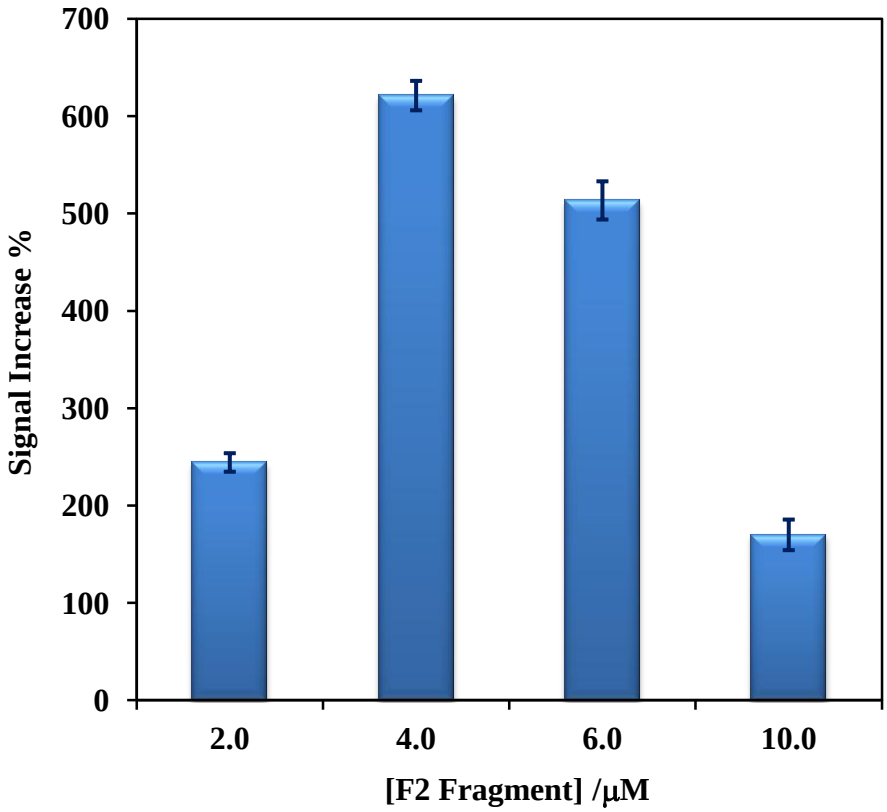

Fig. 8.

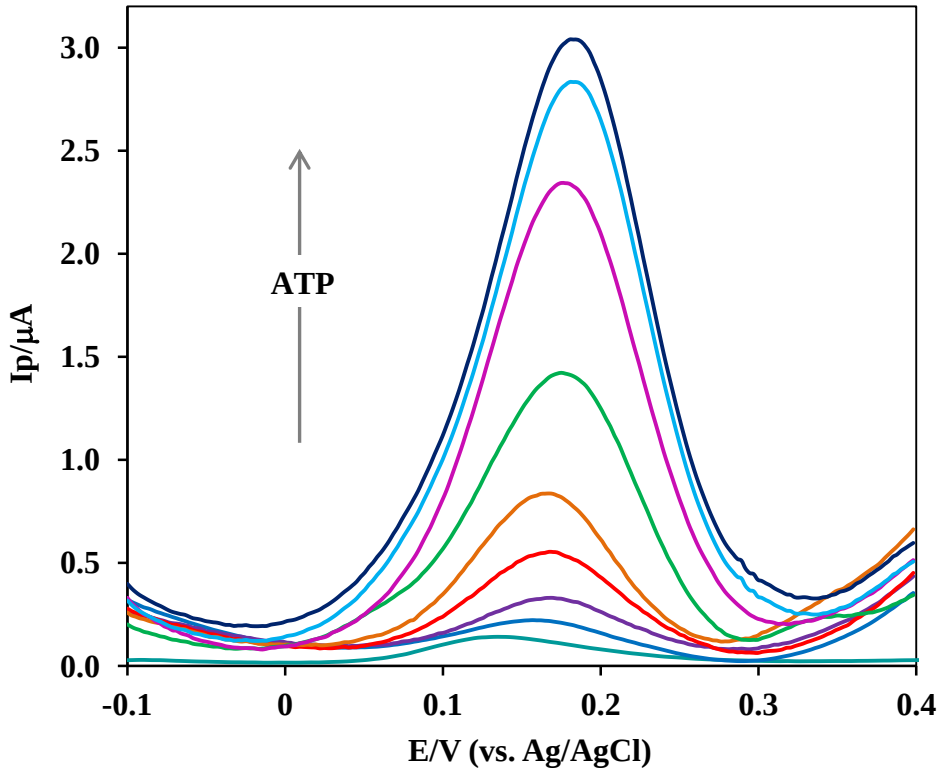

Fig.9.

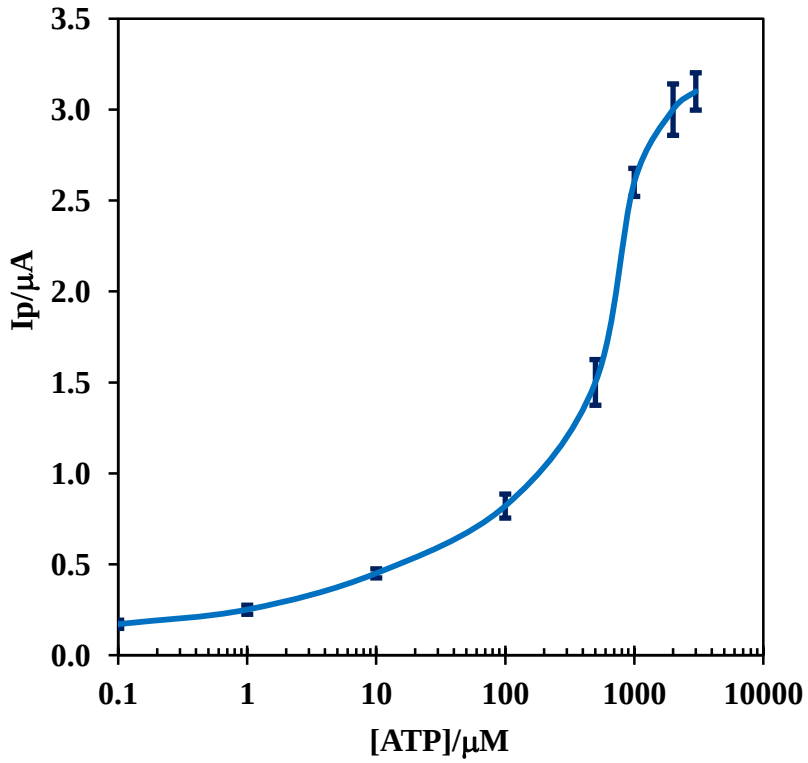

Highlights

- Application of gold nanoporous platforms for the construction of aptasensors is described.
- Nanostructure platforms enhance the detection sensitivity of aptasensors.
- The aptasensor can detect the concentrations of ATP at sub-micromolar scales.
- Very selective response of aptasensor to ATP against the ATP analogues.